TISSUE ENGINEERING: Part A
Volume 22, Numbers 9 and 10, 2016

DOI: 10.1089/ten.tea.2015.0527

termis
Tissue Engineering
& Regenerative Medicine
International Society

ORIGINAL ARTICLE

Small Molecule Inhibition of Transforming Growth Factor Beta Signaling Enables the Endogenous Regenerative Potential of the Mammalian Calvarium

Kshemendra Senarath-Yapa, MA, MBBChir, MRCS,[1–3] Shuli Li, PhD,[1] Graham G. Walmsley, PhD,[1,4] Elizabeth Zielins, MD,[1] Kevin Paik, BS,[1] Jonathan A. Britto, MBBS, MD, FRCS,[5] Agamemnon E. Grigoriadis, PhD,[2] Derrick C. Wan, MD,[1] Karen J. Liu, PhD,[2] Michael T. Longaker, MD,[1,4] and Natalina Quarto, PhD[1,6]

Current approaches for the treatment of skeletal defects are suboptimal, principally because the ability of bone to repair and regenerate is poor. Although the promise of effective cellular therapies for skeletal repair is encouraging, these approaches are limited by the risks of infection, cellular contamination, and tumorigenicity. Development of a pharmacological approach would therefore help avoid some of these potential risks. This study identifies transforming growth factor beta (TGFβ) signaling as a potential pathway for pharmacological modulation *in vivo*. We demonstrate that inhibition of TGFβ signaling by the small molecule SB431542 potentiates calvarial skeletal repair through activation of bone morphogenetic protein (BMP) signaling on osteoblasts and dura mater cells participating in healing of calvarial defects. Cells respond to inhibition of TGFβ signaling by producing higher levels of BMP2 that upregulates inhibitory *Smad6* expression, thus providing a negative feedback loop to contain excessive BMP signaling. Importantly, study on human osteoblasts indicates that molecular mechanism(s) triggered by SB431542 are conserved. Collectively, these data provide insights into the use of small molecules to modulate key signaling pathways for repairing skeletal defects.

Introduction

The incidence of bone pathologies and injuries requiring skeletal repair is rising exponentially. In the United States, more than half million patients per year require repair of bone defects costing more than $2.5 billion, a figure that is due to double by 2020.[1,2] Repair and reconstruction of the craniofacial skeleton constitute a significant portion of this sum, costing more than $585 million.[3] Juxtaposed with burgeoning clinical need are the relatively poor ability of bone healing compared with other tissues and the limitations of current therapeutic approaches to deliver optimal solutions for these clinical challenges. Current surgical techniques to treat craniofacial defects include the use of autologous, allogeneic, and prosthetic materials to achieve bone reconstruction.[4–6] Although autologous bone grafting has provided good results, it is limited by donor site morbidity, scarring, bleeding inflammation, and chronic pain.[7] Furthermore, infection and immunologic rejection are risks for allogeneic bone. Given the dichotomy between the increasing clinical need and the limitations of currently available therapeutic options, the impetus for developing new strategies for bone tissue engineering and for potentiating endogenous bone healing remains high.

An array of signaling pathways orchestrates the maturation and interplay of the key cells involved in bone physiology such as osteoblasts, osteoclasts, and osteocytes.[8,9]

We have previously showed that the disparate embryonic tissue origin of mammalian calvarium[10] leads to significant differences in the activity of key signaling pathways that govern osteogenic and regenerative potential.[11–15] Recently, we have identified that enhanced transforming growth factor beta (TGFβ) signaling in mesoderm-derived parietal bone osteoblasts (PObs) has a key role in determining their elevated

[1]Hagey Laboratory for Pediatric Regenerative Medicine, Department of Surgery, Stanford University School of Medicine, Stanford, California.
[2]Department of Craniofacial Development and Stem Cell Biology, Dental Institute, King's College London, London, United Kingdom.
[3]Department of Plastic and Reconstructive Surgery, North Western Deanery, Manchester, United Kingdom.
[4]Institute for Stem Cell Biology and Regenerative Medicine, Stanford University School of Medicine, Stanford, California.
[5]Department of Craniofacial Surgery, Great Ormond Street Hospital, London, United Kingdom.
[6]Dipartimento di Scienze Biomediche Avanzate, Universita' degli Studi di Napoli Federico II, Napoli, Italy.

apoptotic activity and diminished osteogenic capacity.[16] This finding provides the impetus for our current study, which investigates the possibility of potentiating bone regeneration in the mammalian calvarium through inhibition of TGFβ signaling by employing the small molecule SB431542.[17]

TGFβ, prototype of TGFβ superfamily, is abundant in bone and is a key player in bone turnover and homeostasis.[18–21] Depending on its context, TGFβ can promote or inhibit osteogenesis. Administration of exogenous TGFβ protein has been shown to increase osteogenic markers in human osteoblasts and to be capable of inducing bone formation in periosteum.[22,23] Studies on several *in vivo* bone repair models have also provided evidence for a proosteogenic role for TGFβ.[24–27] Conversely, in immature cells, TGFβ has an inhibitory effect. Alliston *et al.* reported that TGFβ inhibits osteoblast differentiation through Smad3-mediated suppression of Runx2 function and expression.[28] Moreover, overexpression of TGFβ2 in transgenic mice causes osteoporosis.[29]

TGFβ superfamily ligands transduce their signals through two types of serine/threonine kinase receptors.[30–33] Bone morphogenetic proteins (BMPs) bind to Alk-2, Alk-3, and Alk-6, whereas TGFβs and activins bind to Alk-5 and Alk-4. Smads, intracellular signal transducers for TGFβ superfamily ligands, exist as three distinct subclasses: receptor-activated Smads (R-Smads), common-partner Smads (Co-Smads), and inhibitory Smads (ISmads).[30–33]

Small molecule inhibitors are valuable tools for deciphering the roles of signaling pathways in diverse biological processes. Furthermore, they have significant potential for use as clinical therapies.[34–36] SB431542, a specific and potent inhibitor of TGFβ targeting Alk-4, –5, and –7,[17] is undergoing preclinical studies, including anticancer therapies, wound healing, and the treatment of Chagas disease.[37–42]

In this study, using a mouse calvarial defect model, we demonstrate that SB431542 treatment significantly improved bone regeneration *in vivo*. Our results also reveal the presence of cross-talk between TGFβ and BMP signaling, with inhibition of TGFβ signaling by SB4315242 potentiating BMP signaling, both *in vitro* and *in vivo*. Moreover, SB431542 treatment upregulates inhibitory *Smad6* expression in response to elevated production of BMP2 ligand, thus providing a negative feedback loop to contain excessive BMP signaling. Interestingly, studies on human osteoblasts indicate that the molecular mechanism(s) through which SB431542 inhibition of TGFβ signaling enhances bone repair is conserved among species. Therefore, this study provides insights into the potential therapeutic applications of small molecule inhibitors to treat human craniofacial skeletal defects either in isolation or as an adjunct to current therapeutic approaches.

Materials and Methods

Animals

All animal experiments were performed in accordance with the Stanford University Animal Care and Use Committee Guidelines (APLAC 9999); postnatal day 10 (pN10) CD-1 mice (Charles Rivers Laboratories, Inc.) were used for this study. Two-millimeter defects were made in the parietal bone of CD-1 mice ($n=5$) as previously described.[43–45] In brief, after anesthesia and disinfection, a longitudinal incision of the skin was made. The pericranium was removed and 2-mm calvarial defects were created in the parietal bone of pN10 mice with a trephine drill and meticulous care to avoid damaging underlying dura mater (DM). Parietal bone defects were treated with a 1.5-mm-diameter collagen sponge (Helistat; Integra LifeSciences Cooperation) soaked in 1 μL of 26 mM SB431542 (Sigma-Aldrich), 400 ng of human recombinant TGFβ1 (R&D Systems, Inc.) in 1 μL phosphate-buffered saline (PBS), 1 μL dimethylsulfoxide (DMSO), or 1 μL PBS as a control. Of note, dose of SB431542 was chosen based on a dose–response pilot assay, with 26 mM being the most effective in repairing the calvarial defects without any toxicity for the tissue. The collagen sponge acted as a vehicle to deliver the molecule to the sight of the injury.

The skin incision was then closed and mice were allowed to recover. Subcutaneous injections of SB431542 were given on alternate days for a period of 2 weeks at the site of the defect at the concentrations as mentioned in a volume of 100 μL. The site of the defect was marked with 10.0 Ethilon sutures at skin level.

Micro-computed tomography imaging

Micro-computed tomography (μCT) imaging was performed as previously described.[14] Mice underwent μCT scanning on a weekly basis from 1 to 8 weeks ($n=5$) for each treatment. μCT was performed using a high-resolution MicroCAT II™ (ImTek, Inc.) small animal imaging system, with previously described settings.[46] Two-dimensional projection images were used to reconstruct tomograms with a commercial software package (Cobra EXXIM; EXXIM Computing Corp.), resulting in a resolution of 80 μm. Three-dimensional reconstructions were generated by MicroView software (GE Healthcare). Each mouse was scanned with a CT phantom, which was used to calibrate each scan. The precise threshold for regenerating calvarial bone was previously determined as equivalent to 510 Hounsfield Units. The rest-defect area was then determined with the Magic Wand Tool in Photoshop (Adobe Systems). Percentage healing was determined by dividing the rest-defect area by the mean of the defect size one day postoperatively. Student's test was used for statistical analyses. A p value <0.05 was considered statistically significant.

Mouse tissue harvesting and primary cell culture

Mesoderm-derived PObs were harvested from skulls of (pN10) mice to match the age of mice enrolled in the *in vivo* calvarial defect surgeries. The periosteum and DM were carefully stripped off from the skull and dural membranes were collected in cold PBS on ice for dural cell harvest. The peripheral suture complexes of each frontal or parietal bone were also carefully removed. Parietal bones were minced separately into small chips less than 1 mm before digestion. Parietal bone chips were digested with 0.2% Dispase II and 0.1% Collagenase A (Roche Diagnostics) in serum-free medium. The digestion was carried out six times, each for 10 min. The first two digestions were discarded. The later four digestions were pooled together. All digestions were neutralized with an equal volume of α-minimum essential medium (α-MEM) supplemented with 10% fetal bovine serum (FBS), 100 IU/mL penicillin and streptomycin (Gibco Life Technologies and Invitrogen Corporation), pelleted and resuspended in the growth medium (GM). POb cells were plated in 100 mm tissue culture dishes (Corning Incorporated) and incubated at 37°C

with continuous supplement of 5% CO_2. The medium was changed every other day. Only passage 0–3 cells were used for all experiments. For DM cells, dural membranes were collected and washed in cold PBS and dilute Betadine. After 10 min incubation at 37°C in 0.05% trypsin, digested membranes were placed in 100 mm tissue culture dishes and cultured with Dulbecco's modified Eagle's medium (DMEM) supplemented with 10% FBS and 100 IU/mL penicillin and streptomycin. Only passage 0–3 cells were used for experiments.

Human calvarial bone harvesting and primary cell culture

Human calvarial bone samples were obtained according to Stanford Institutional Review Board guidelines (IRB 28853). Bone chips that would otherwise be discarded after the procedure were obtained from children undergoing preplanned calvarial bone grafting procedures at Lucile Packard Children Hospital. Bone chips were taken from the peripheries of the sample and separated from the suture itself. All patients were between 3 and 6 months of age. Under sterile conditions, periosteum was stripped of and the chips were washed with dilute Betadine and PBS before digestion according to the murine osteoblast protocol already described. DMEM supplemented with 10% FBS and 100 IU/mL penicillin and streptomycin was used for all human primary cell cultures. Only early passage (1–3) cells were taken for all experiments.

Osteogenic differentiation assay and alizarin red staining

POb cells were plated in six-well plates (1×10^5/well). Upon subconfluence, cells were incubated with the osteogenic differentiation medium (ODM), composite of either α-MEM or DMEM supplemented with 10 μM glycerol β-phosphate, 0.25 μM ascorbic acid (Sigma-Aldrich), 10% or 3% FBS, and 100 IU/mL penicillin and streptomycin. The medium was changed every other day. Differentiation assays were also performed in the presence of SB431542 (10 μM; Sigma-Aldrich), recombinant mouse noggin (250 ng/mL) or DMSO (1:1000) as a control (R&D Systems). Mineralization of the extracellular matrix was assessed by alizarin red staining and quantification at days 21–28 of the differentiation as previously described.[46]

RNA isolation, reverse transcription, and quantitative real time polymerase chain reaction

Total RNA isolation, reverse transcription-polymerase chain reaction (RT-PCR), quantitative PCR (qPCR), primers sequence for mouse and human *Runx2*, *Bglap*, and *Gapdh*, and annealing temperature were previously described.[11,13,47] Specific primers for *Bmp2* and *Smad6* and *Id2* were designed based on their GenBank sequence, and sequences are as follows: m*Smad6*Fwd:TACCACTTCAGCCGGCCTCTG; m*Smad6*Rev:AGTACGCCACGCTGCACCAGT; m*Bmp2*Fwd:ACCCGCTGTCTTCTAGTGTTG; m*Bmp2*Rev:TCTCTGCTTCAGGCCAAACA; m*Id2*Fwd:GATGATCGTCTTGCCCAGGT; m*Id2*Rev:TCTGGTATTCACGCTCCACC annealing at 57°C. *hSMAD6*Fwd:CCCCCGGCTACTCCATCAAGGTGT; *hSMAD6*Rev:GTCCGTGGGGGCTGTGTCTCTGG; annealing at 65°C.

Measurement of Caspase 3 activity

The Caspase 3 fluorometric protease assay was performed using a Caspase 3 Apoptosis Detection Kit (sc-4263 AK; Santa Cruz Biotechnology) as previously described protocols.[16] Cells were collected at different time points of osteogenic differentiation, 40 μL of cell lysate (in triplicate) was incubated with 200 μL of reaction buffer, 5 μL of Ac(N-acetyl)-DEVD-AFC(7-amino-4-trifluoromethylcoumarin) (EDVD-AFC) substrate, and dithiothreitol (DTT) (10 μM final concentration). The reaction was incubated at room temperature for 1 h. The analysis was conducted using a fluorescent microplate reader (SpectraMAX Gemini XS; Molecular Devices Corporation) at excitation/emission wavelength of 400/505 nm. Levels of emission of POb and dural cells with or without SB431542 treatment were compared.

Immunoblotting analysis

POb and DM cells were collected at different time points of osteogenic differentiation assay performed with or without either SB431542 or TGFβ. Cells were lysed with cold RIPA buffer (50 mM of HEPES, pH 7.5, 150 mM of NaCl, 1 mmol/ of ethylenediaminetetraacetic acid (EDTA), 10% glycerol, 1% Triton X-100, 25 mM sodium fluoride) containing 1 mM sodium orthovanadate and Proteases Inhibitor Cocktail (Sigma-Aldrich). Cell lysates (40 μg) were electrophoresed on 12% Tris-HCl sodium dodecyl sulfate (SDS)-PAGE gels (Precast Nupage gels; Gibco Life Technologies and Invitrogen Corporation) and transferred onto Immobilon-P membrane (Millipore Corporation). Immunoblotting analysis was performed using the following primary rabbit antibodies: anti-pSmad2/3 (Ser465/467), anti-Smad2/3, anti-pSmad1/5 (Ser465/467), anti-Smad1/5 (1:500; Cell Signaling), and anti-α-tubulin (1:1000; ab8227; Abcam). A second horseradish peroxidase-conjugated antirabbit antibody was used (1:3000; Cell Signaling). Immunoblotted proteins were observed by enhanced chemiluminescence (Amersham Biosciences). To assess for the total amount of endogenous Smad2/3 and Smad1/5, and to control for equal loading and transfer of the samples, the membranes were reprobed with anti-Smad2/3, anti-Smad1/5 antibodies, and anti-α-tubulin antibody. Densitometry analysis of electrophoretic bands was performed using the ImageJ software program (NIH). The densities of pSmad2/3 and pSmad1/5 bands were normalized to the loading controls (α-tubulin) and presented as percentage increase. The results are the mean ± standard deviation (SD) of three independent experiments.

Preparation of cell-conditioned media

Cell-conditioned media (CM) were obtained from cells undergoing osteogenic differentiation with and without SB431542. At day 4 of osteogenic differentiation, cells were washed three times with sterile PBS before addition of 5 mL ODM supplemented with 1% serum. After 48 h, CM were collected and concentrated 100-fold using Centricon filters (Centricon-3, 3000 NMWL; Millipore Corporation). The volume of each CM was normalized by cell numbers so that an equal volume of medium was produced by an equal number of cells. CM for the TGFβ enzyme-linked immunosorbent assay (ELISA) were collected from POb and DM cells cultured in DMEM supplemented with 1% serum. Collection

and concentration of CM were carried out at 4°C. Protein concentration of each medium was determined by bicinchoninic acid (BCA) protein assay (Pierce). Equal amount of total proteins from each medium was analyzed for TGFβ1 and BMP2 levels as described hereunder. All experiments were performed twice using freshly harvested media.

Enzyme-linked immunosorbent assay

Endogenous levels of TGFβ1 and BMP2 were analyzed on conditioned medium (100 μg total protein) by ELISA (Quantakine DB100B and DBP200; R&D Systems) according to the manufacturer's instruction. Photometric detection was done at 420-nm wavelength. Each sample was run in triplicate. The assay was repeated twice.

Histology

Eight weeks after surgery, after sacrifice of mice by CO_2 asphyxiation, calvaria were harvested, fixed in 0.4% paraformaldehyde (PFA), and decalcified in 19% EDTA at 4°C for 2 weeks. Specimens were then embedded in paraffin, cut into 8-μm sections, and stained with a modified Movat's Pentachrome procedure.[48] Sections were examined using a Carl Zeiss Axioplan 2 (Zeiss) microscope. Images were captured by AxioVision (Zeiss) and combined by Adobe Photoshop (Adobe Systems).

Immunohistochemistry

Immunohistochemistry was performed on calvariae harvested at 24, 48, and 72 h and day 6 postsurgery. Specimens were fixed in 0.4% PFA overnight, decalcified, processed for optimal cutting temperature frozen section embedding, and cut into 8-μm sections. For all other immunohistochemistry, antigen retrieval was performed by incubating the slides with Proteinase K (Sigma-Aldrich) at 37°C for 10 min. Primary rabbit antibodies pSmad2/3 and pSmad1/5 antibodies (Cell Signaling Technology) were used at a dilution of 1:50. Dilution for rabbit Smad6 antibody (Sigma-Aldrich) was 1:100. Alexa Fluor 488 goat antirabbit IgG was used as secondary antibody (Life Technologies). Frozen sections incubated with a primary nonimmune IgG antibody diluted at 1:100 (Rabbit IgG Control #10500C; Thermo Scientific) followed by incubation with Alexa Fluor 488 goat antirabbit IgG secondary antibody were used as negative control. Results were obtained from at least three animals per time point and immunohistochemistry was carried out in triplicate.

Statistical analysis

Data are expressed as mean ± SD of three independent experiments. The error bars in the graphs represent 1 SD. Statistical differences between the means are examined by Student's test. A p value <0.05 was considered statistically significant.

Results

In vivo *inhibition of TGFβ signaling with the small molecule inhibitor SB431542 enhances calvarial regeneration*

Previous work from our group has established (1) that the different embryonic tissue origin of calvarial bones influences their osteogenic potential and tissue regeneration and (2) that differential activation of fibroblast growth factor (FGF), canonical WNT, and BMP pathways is responsible for these regional differences with enhanced activity of proosteogenic signaling in frontal bone and derived osteoblasts.[11–13,16] More recently, we have identified that the TGFβ pathway has enhanced activity in paraxial mesoderm-derived PObs and, furthermore, that this correlated with increased apoptotic activity in POb cells.[16] That study also indicated a reciprocal relationship between apoptotic activity and osteogenic capacity and demonstrated that inhibition of TGFβ signaling with the small molecule inhibitor SB431542[17] increased osteogenic differentiation of POb cells *in vitro*.[16] Therefore, we began this study to investigate whether these *in vitro* findings would translate into enhanced potential for calvarial healing *in vivo,* upon administration of SB431542 in mouse calvarial defects. For this aim, 2-mm calvarial defects were created in the parietal bone of pN10 mice as previously described.[49] A collagen sponge was then placed into the defect with either 200 μL of 26 mM SB431542 or 200 μL of vehicle DMSO, which served as a control. After surgery, μCT analysis was performed at different time points (Fig. 1A, B). As early as week 1, there was a significantly increased rate of calvarial healing in the SB431542 treatment group (61.9% ± 6.5%, $n=5$) versus the control DMSO group (24.5% ± 6.5%, $n=5$). This statistically significant difference in the two healing curves ($p<0.05$) persisted into week 6 at which point the SB431542 healing was 73.6% ± 8.9% and the DMSO control group healing was 49.8% ± 9.0% (Fig. 1B). In marked contrast, TGFβ treatment reduced calvarial healing compared with untreated controls, thus confirming the beneficial effect of inhibiting TGFβ signaling for bone repair (Fig. 1C). To ensure that our SB431542 treatment was effectively inhibiting TGFβ signaling *in vivo*, coronal sections of calvaria defects were harvested at 24 and 72 h postsurgery and analyzed by immunohistochemistry for endogenous levels of pSmad2/3, a downstream effector of TGFβ signaling (Fig. 1D). We analyzed the dural membrane spanning the defect for pSmad2/3 positive staining, because it has been previously shown that, upon creation of calvarial defects, at early time points DM cells migrate into the area of defects and contribute significantly to endogenous calvarial healing.[14] In representative images taken from mice treated with SB431542, or DMSO, it can be seen that as early as 24 and 72 h, our treatment was effectively suppressing TGFβ signaling, as demonstrated by reduced pSmad2/3 staining in the SB431542-treated group as compared with control group (Fig. 1D). To assess the extent of bony regenerate, histologically, coronal sections of skulls at 8 weeks postsurgery were stained using pentachrome procedure. This staining confirmed superior healing capacity in SB431542-treated groups compared with DMSO control as indicated by marked bone matrix formation (Fig. 1E and right panel showing higher magnification of boxed area). Moreover, ELISA indicated that DM cells produce significantly higher levels of TGFβ1 than POb cells (Fig. 1F).

Inhibition of TGFβ signaling increases osteogenic capacity and reduces apoptotic activity of DM cells

It has previously been established that DM cells play a key role in endogenous calvarial healing.[49–51] Therefore, we

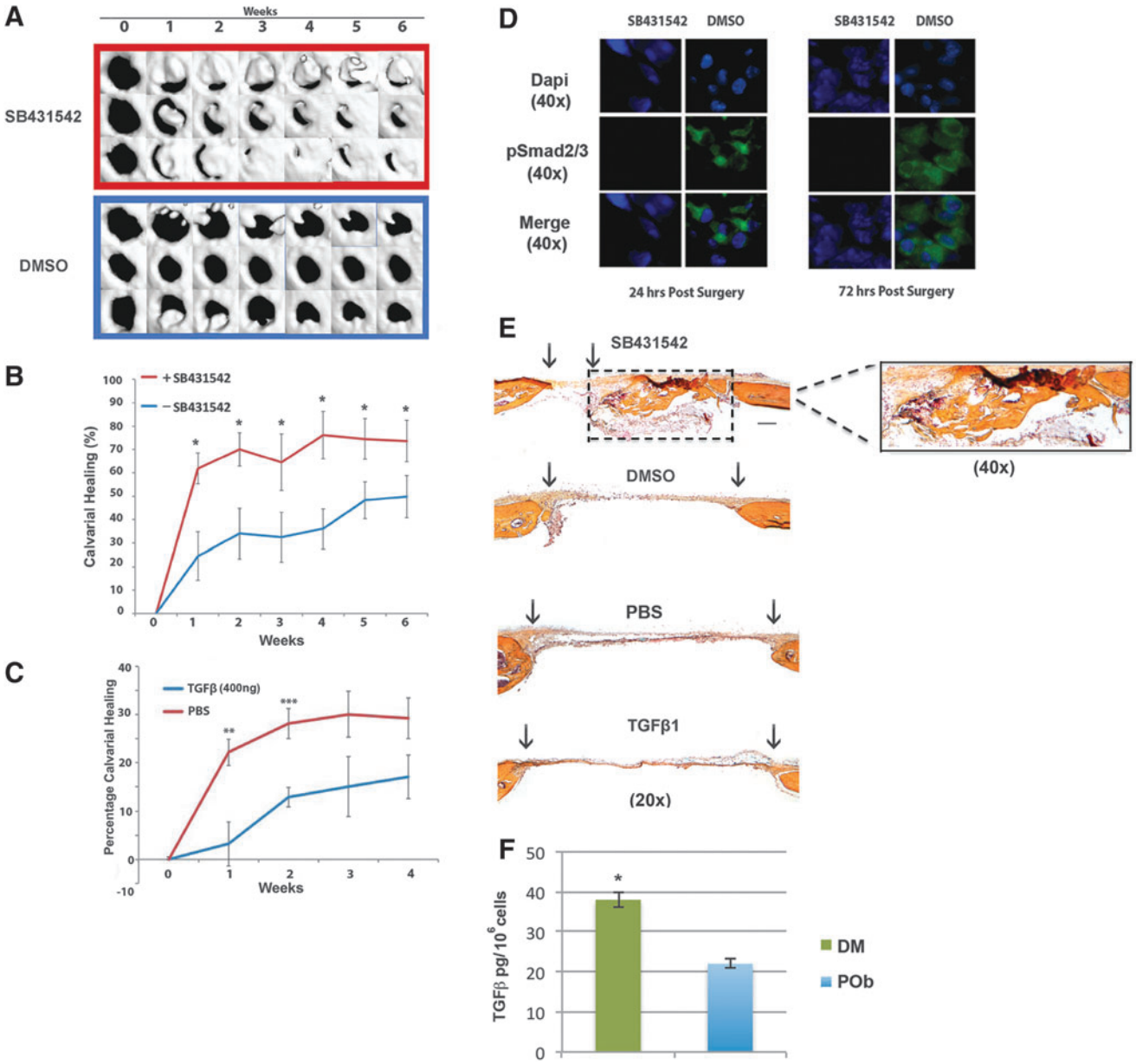

FIG. 1. Inhibition of TGFβ signaling using the small molecule inhibitor SB431542 accelerates healing of calvarial defects in parietal bone. **(A)** Time course of three representative mouse parietal defects treated with SB431542 or DMSO (control treatment and solvent for SB431542). **(B)** Quantification of defect repair ($n=5$) according to μCT results analyzed using magic wand tool in Photoshop after standardization of threshold for regenerating calvarial bone. **(C)** Quantification of calvarial healing by μCT in TGFβ (400 ng)-treated calvarial defects ($n=5$) versus PBS controls shows significant reduction in the healing rates 1-week ($p<0.01$) and 2-week ($p<0.001$) postsurgery. At later stages, differences persisted with TGFβ-treated groups healing less than untreated group. **(D)** Indirect immunofluorescence for pSmad2/3, a downstream effector of TGFβ signaling, performed on coronal sections through DM spanning the calvarial defect shows effective inhibition of TGFβ signaling *in vivo* at 24 and 72 h after calvarial defect surgery. **(E)** Pentachrome staining of coronal sections of skull defect at postsurgery at week 8 showing significant differences in calvarial repair between SB431542-treated defects and control as well TGFβ-treated and corresponding PBS control. Bony tissue regenerate is observed in SB431542-treated defects as shown in *yellow*. *Right panel* is a higher magnification (40×) of *dashed box*, showing new formed bony tissue in SB431542-treated calvarial defects. Scale bar: 100 μm. **(F)** ELISA indicates that DM cells elaborate significantly higher amount of TGFβ protein than POb cells. $*p\leq0.05$; $**p\leq0.01$; $***p\leq0.001$. DM, dura mater; DMSO, dimethylsulfoxide; ELISA, enzyme-linked immunosorbent assay; μCT, micro-computed tomography; PBS, phosphate-buffered saline; POb, parietal bone osteoblast; TGFβ, transforming growth factor beta. Color images available online at www.liebertpub.com/tea

investigated the impact of inhibition of TGFβ signaling on the osteogenic capacity of these cells. Cells were grown in ODM for 21 days supplemented with either 10 μM SB431542 or the equivalent concentration of DMSO alone as control. The cells were then stained with 0.2% alizarin red to assess the mineralization of the extracellular matrix. As shown in Figure 2A, SB431542-treated cells stained more robustly than the control group, indicating that inhibition of TGFβ signaling enhanced osteogenic differentiation. Quantification of alizarin red staining confirmed increased mineralization in SB431542-treated cells (Fig. 1B). In contrast, DM cells grown in GM for 21 days supplemented with either 10 μM SB431542 or the equivalent concentration of DMSO did not show extracellular matrix mineralization. Immunoblotting analysis of cell lysates taken at different time points during osteogenic differentiation revealed effective inhibition of TGFβ signaling as signified by reduced pSmad2/3 (Fig. 2C, lower panel). Furthermore, molecular analysis of specific osteogenic markers showed enhanced osteocalcin (*Bglap*) expression at late time points with a significantly higher level at day 12 and day 18 in SB431542-treated cells (Fig. 2D). *Runx2* expression was also higher in the SB431542-treated

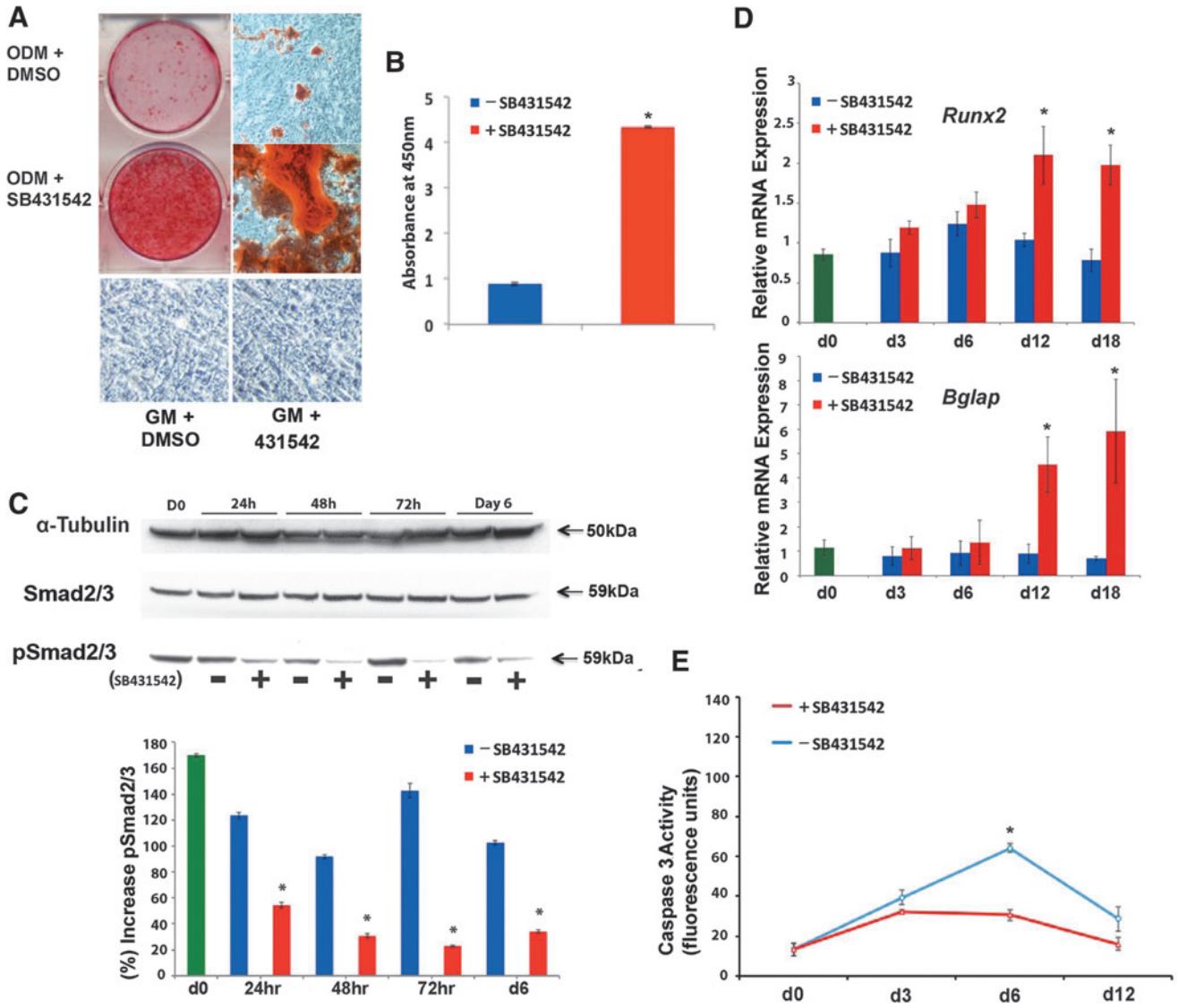

FIG. 2. Inhibition of TGFβ signaling by SB431542 in DM cells enhances osteogenic capacity and protects from apoptosis. **(A)** Mineralization of the extracellular matrix detected by alizarin red staining. Of note, DM cells cultured in GM with or without SB431542 treatment did not show extracellular matrix mineralization. **(B)** Alizarin red quantification shows significantly increased osteogenic differentiation in SB431542-treated cells compared with DMSO controls. **(C)** Immunoblotting analysis of pSmad2/3, pan-Smad2/3, and α-tubulin. Quantification of electrophoretic bands (*lower panel*) using the ImageJ software program reveals effective inhibition of TGFβ signaling at different time points during osteogenic differentiation. Representative blot of three independent experiments. **(D)** Gene expression analysis of early and late osteogenic markers such as *Runx2* and osteocalcin (*Bglap)* examined by qPCR shows that treatment with SB431542 upregulates *Runx2* and *Bglap* expression. The relative mRNA level in each sample is normalized to *Gapdh*. **(E)** Time course Caspase 3 activity performed on DM cells undergoing osteogenic differentiation with or without SB431542 demonstrates reduced apoptotic activity in treated cells. $*p \leq 0.05$. GM, growth medium; ODM, osteogenic differentiation medium; qPCR, quantitative polymerase chain reaction. Color images available online at www.liebertpub.com/tea

group at all time points (Fig. 2D). Taken together, these data indicate that *in vitro* inhibition of TGFβ signaling enhances the osteogenic potential of DM cells.

Given that TGFβ signaling has been implicated in promoting apoptosis in a number of different tissue types and that we have previously demonstrated that TGFβ inhibition reduces apoptosis in murine POb cells,[16] we next investigated the effect of this treatment on apoptotic activity in DM cells.

An osteogenic differentiation assay was performed in the presence or absence of SB431542, and cell lysates were analyzed for Caspase 3 activity, a key apoptotic protease. As shown in Figure 2E, SB431542 treatment reduced apoptotic activity with a significant difference ($p < 0.05$) at day 6. Similar results were observed when SB431542 treatment was applied to POb cells (data not shown), thus confirming previous findings[16] and indicating that the effect of SB431542 treatment on DM cells mirrored that observed on POb cells.

Inhibition of TGFβ signaling potentiates BMP signaling and demonstrates the presence of cross-talk between these pathways

Treatment with SB431542 has previously been shown to promote osteogenic differentiation in immortalized osteoblasts. Interestingly, these treatments concurrently led to phosphorylation of BMP-specific RSmads, such as Smad1/5, implying the presence of cross-talk between the TGFβ and BMP pathways.[52] Therefore, we first sought to establish the presence of cross-talk in primary cultures of DM cells and POb cells *in vitro*. Cell lysates were collected from both cells undergoing osteogenic differentiation with and without SB431542 and analyzed for endogenous pSmad2/3 and pSmad1/5 by the immunoblotting technique. SB431542 treatment effectively decreased endogenous pSmad2/3 levels in both DM cells (Fig. 3A) and POb cells (Fig. 3B), signifying successful inhibition of TGFβ signaling. Conversely, SB431542 treatment led to increased pSmad1/5 level at 24 and 48 h (Fig. 3C, D). The effect was significant ($p < 0.05$) at 48 h for both DM cells (Fig. 3C) and POb cells (Fig. 3D). Moreover, SB431542 treatment upregulated the expression of *Id2* (Fig. 3E, F), a direct target of Smad1/5[53], thus further confirming the activation of the BMP signaling pathway.

Collectively, these data support the existence of cross-talk between the TGFβ and BMP signaling pathways during osteogenic differentiation either in DM or in POb cells.

Having demonstrated the presence of cross-talk between the TGFβ and BMP signaling pathways *in vitro*, we then examined potential *in vivo* cross-talk between these pathways. Coronal sections of calvaria harvested from mice at 24 and 72 h postsurgery were analyzed for endogenous pSmad2/3 and pSmad1/5 by indirect immunofluorescence. Administration of SB431542 effectively suppressed TGFβ signaling *in vivo*. Figure 4A shows representative images taken of DM cells that span the defect. Intense nuclear immunofluorescent staining is seen for pSmad2/3 at both 24 and 72 h in all treatment groups except the SB431542 group, in which nuclear staining significantly reduced at both 24 and 72 h. Figure 4B illustrates quantification of the percentage of nuclei positive for pSmad2/3 calculated from six different fields of DM spanning each entire defect. Taken together, these data demonstrate that treatment with SB431542 suppressed pSmad2/3 and, therefore, TGFβ signaling *in vivo*. Conversely to its inhibitory effects on TGFβ signaling, administration of SB431542 potentiated BMP signaling, resulting in a more sustained BMP response. Representative images taken of DM cells that span the defect showed intense nuclear immunofluorescent staining for pSmad1/5 at 24 and 72 h, indicating that although at 24 h there is active BMP signaling in all treatment groups, by 72 h, BMP signaling activation waned in all groups with the exception of SB431542 (Fig. 4C). Thus, administration of SB431542 sustained the endogenous activation of BMP signaling, as indicated also by quantification of the percentage of pSmad1/5 positive nuclei (Fig. 4D). Collectively these data reveal a cross-talk between the TGFβ and BMP pathways, thus providing one possible explanation for the enhanced calvarial healing observed in the SB431542 treatment group relative to DMSO controls.

Upregulation of Smad6 *expression in response to elevated production of BMP2 in SB431542 cells provides a negative feedback loop to contain excessive BMP signaling*

Downregulation of inhibitory Smad6 has been previously suggested as a mechanism for cross-talk between the TGFβ and BMP signaling pathways.[52] To investigate whether a similar mechanism may be in play in DM and POb cells, we performed an expression profile of *Smad6* during osteogenic differentiation. As shown by PCR analysis, SB431542 treatment led to an unexpected *Smad6* upregulation rather than the expected downregulation. Increased *Smad6* expression upon TGFβ inhibition was seen in both osteoblasts and DM cells (Fig. 5A, B), thus ruling out the possibility of reduced *Smad6* as being the underlying mechanism for the enhanced BMP signaling observed upon TGFβ inhibition by SB431542.

Given the presence of BMP-responsive element in the promoter of *Smad6,*[54,55] we next investigated whether the *Smad6* upregulation we observed might be a response to elevated BMP signaling, essentially acting as a negative feedback loop to contain excessive BMP signaling. Indeed, POb and DM cells treated with SB431542 expressed increased levels of BMP2 ligand compared with untreated cells as revealed by both PCR analysis (Fig. 5C, D) and ELISA performed on conditioned media collected from cells at day 6 of differentiation (Fig. 5E, F). Furthermore, the *Smad6* upregulation in response to SB431542 treatment was abrogated by addition of noggin (250 ng/mL) (Fig. 5G, H). The latter result suggests that *Smad6* upregulation was indeed a response to elevated BMP signaling and, therefore, that a potential reduction in *Smad6* was not responsible for the elevated BMP signaling in response to SB431542 as initially hypothesized. In contrast, our data demonstrate that the production of elevated level of BMP2 ligand by SB431542-treated cells is responsible for a concerted activation of BMP signaling and upregulation of *Smad6,* with the latter providing a negative feedback loop containing excessive BMP signaling. The occurrence of increased Smad6 in response to SB431542 treatment was also confirmed *in vivo* by immunofluorescence staining on calvarial defects (Fig. 5I, J). As expected, noggin treatment suppressed also the enhanced osteogenic differentiation elicited by SB431542 treatment (Supplementary Fig. S1; Supplementary

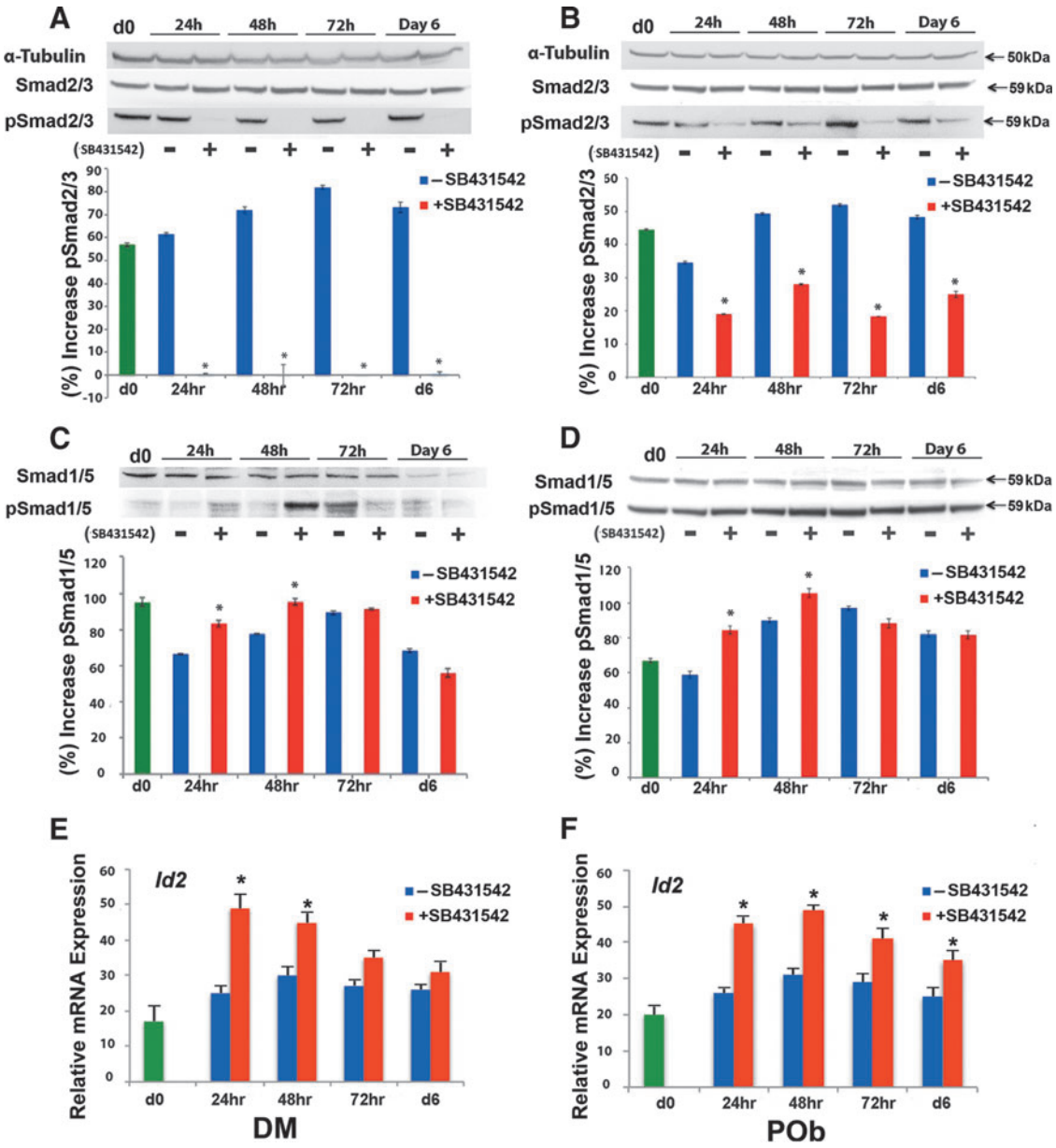

FIG. 3. *In vitro* cross-talk between the TGFβ and BMP signaling pathways. **(A)** Treatment of DM cells undergoing osteogenic differentiation with SB431542 leads to effective inhibition of TGFβ signaling as demonstrated by reduced pSmad2/3 at all time points. Quantification of electrophoretic bands (*lower panel*) is as already mentioned. Membranes were stripped and reprobed with α–tubulin antibody to control for equal loading. Total Smad2/3 proteins were detected by specific anti-pan Smad2/3 antibody. **(B)** SB431542 treatment inhibits TGFβ signaling also in POb cells undergoing osteogenic differentiation as indicated by reduced endogenous pSmad2/3 at all time points. *Lower panel* shows quantification of electrophoretic bands. **(C)** SB431542 treatment of DM cells undergoing osteogenic differentiation increases significantly endogenous pSmad1/5, at 24 and 48 h, signifying increased activation of BMP signaling. Quantification of pSmad1/5 electrophoretic bands (*lower panel*). Membranes were stripped and reprobed with α–tubulin antibody to control for equal loading. Total Smad1/5 proteins were detected by specific anti-pan Smad5 antibody. **(D)** SB431542 treatment leads to increase of endogenous pSmad1/5 also in POb cells. Quantification of pSmad1/5 electrophoretic bands (*lower panel*). Representative blots of three independent experiments. **(E)** qPCR analysis reveals upregulation of the pSmad1/5 target gene, *Id2* in DM cells treated with SB431542 supporting further the activation of BMP signaling. **(F)** Similarly, an upregulation of *Id2* expression is observed also in SB431542-treated POb cells. $*p \leq 0.05$. BMP, bone morphogenetic protein. Color images available online at www.liebertpub.com/tea

Data are available online at www.liebertpub.com/tec) as a result of its inhibitory activity on BMP2 ligand. These data provide further strength to the observation that the enhanced osteogenic differentiation in SB431542-treated cells is a result of increased BMP signaling.

Molecular mechanism(s) triggered by SB431542 are conserved in primary human osteoblasts

To investigate the potential translational benefit of SB431542 treatment in the context of large calvarial defects

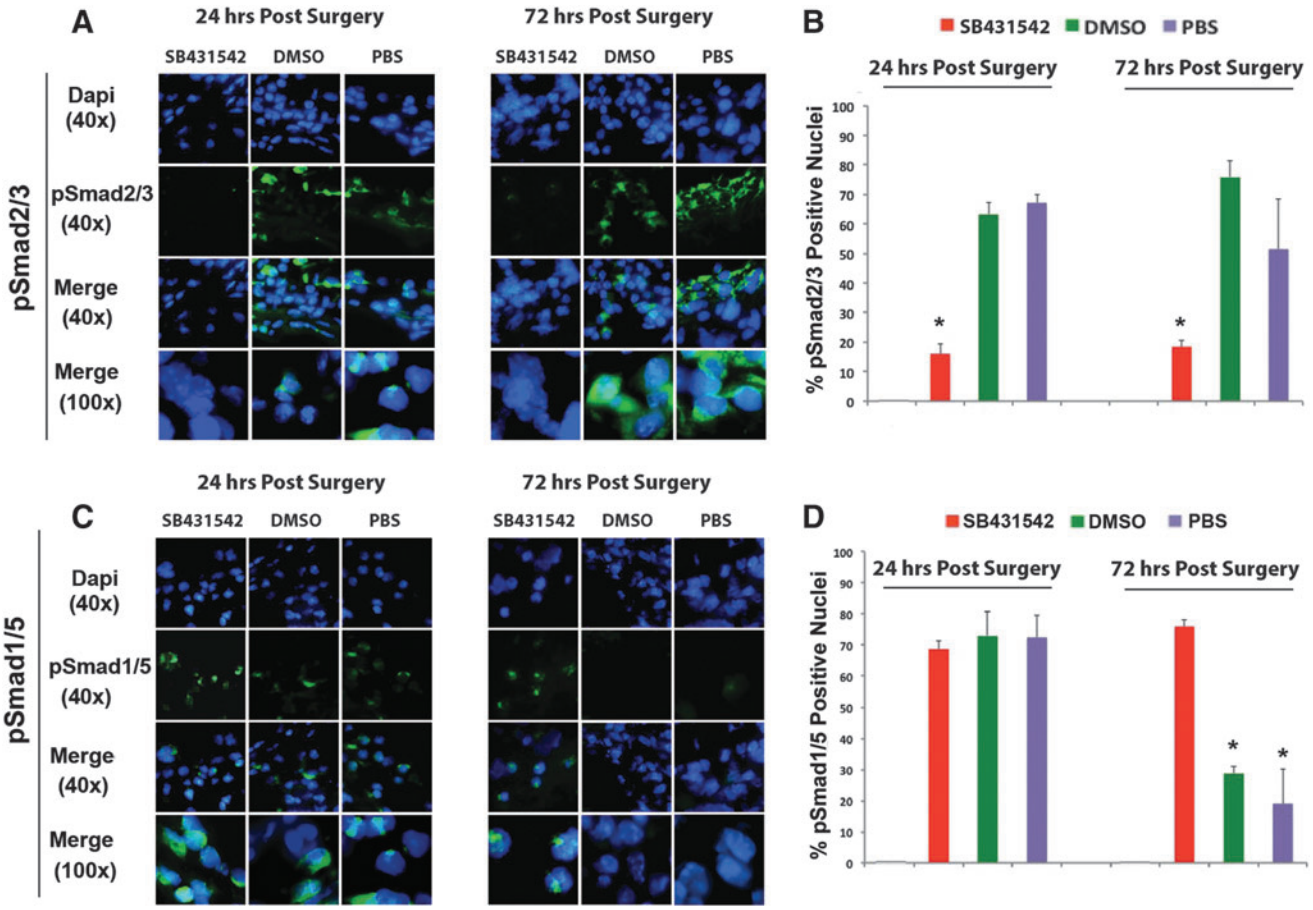

FIG. 4. *In vivo* cross-talk between the TGFβ and BMP signaling pathways in dural tissue spanning calvarial defects. **(A)** Indirect immunofluorescence for pSmad2/3 performed on coronal sections through dura tissue spanning the calvarial defect shows effective suppression of TGFβ signaling *in vivo* at 24 and 72 h after calvarial defect surgery. **(B)** Quantification of the percentage pSmad2/3 positive nuclei in dura tissue spanning the calvarial defect showing a significant reduction of pSmad2/3 positive nuclei at both 24 and 72 h upon treatment with SB431542. **(C)** Indirect immunofluorescence for pSmad1/5, performed on coronal sections through dura spanning the calvarial defect, indicates a more sustained BMP response in the SB431542 treatment group. By 72 h, only the group treated with SB431542 had significantly elevated pSmad1/5. **(D)** Quantification of the percentage pSmad1/5 positive nuclei in dura spanning the calvarial defect showing a persistent increase of pSmad1/5 positive nuclei in SB431542-treated cells, and, therefore, activation of BMP signaling at both 24 and 72 h in the presence of SB431542. Representative blots of three independent experiments. $*p \leq 0.05$. Color images available online at www.liebertpub.com/tea

in human patients, we next investigated the impact of SB431542 treatment on osteogenic capacity of human calvarial osteoblast primary cultures derived from parietal bones (hPOb). To this aim, an osteogenic differentiation assay was performed on hPOb with and without SB431542. This treatment enhanced extracellular mineralization of hPOb compared with untreated cells (Fig. 6A, B), indicating that inhibition of TGFβ signaling also enhances differentiation of human osteoblasts. Furthermore, qPCR analysis of osteogenic markers revealed higher expression of *RUNX2* and *BGLAP* in SB431542-treated cells as compared with controls (Fig. 6C). Immunoblotting analysis of pSMAD2/3 on cell lysates from different time points of osteogenic differentiation showed the effective inhibition of TGFβ signaling by SB431542 (Fig. 6D), while potentiating BMP signaling as demonstrated by elevated pSMAD1/5 (Fig. 6E). This effect was most striking at 72 h as opposed to the 48 h observed in the murine studies. In addition, we observed higher *BMP2* and *SMAD6* expression also in SB431542-treated hPOb (Fig. 6F, G), with noggin abrogating upregulation of *SMAD6* (Fig. 6G). These results indicate that the molecular mechanism(s) underlying the calvarial bone regenerative potential is conserved across species.

Discussion

In this study, by employing an established calvarial defect model, we demonstrate that local administration of SB431542 can promote more robust skeletal repair *in vivo*. By performing immunofluorescence for pSmad2, on coronal sections of treated calvaria, we prove effective inhibition of TGFβ signaling *in vivo*, and we show significant differences in rates of healing between SB431542-treated and untreated defects. As indicated by μCT and histological analysis, the healing rate of defects treated with SB431542 was significantly higher than control groups. To our knowledge, this is the first evidence showing that *in vivo* inhibition of TGFβ signaling promotes skeletal repair through activation of the BMP pathway.

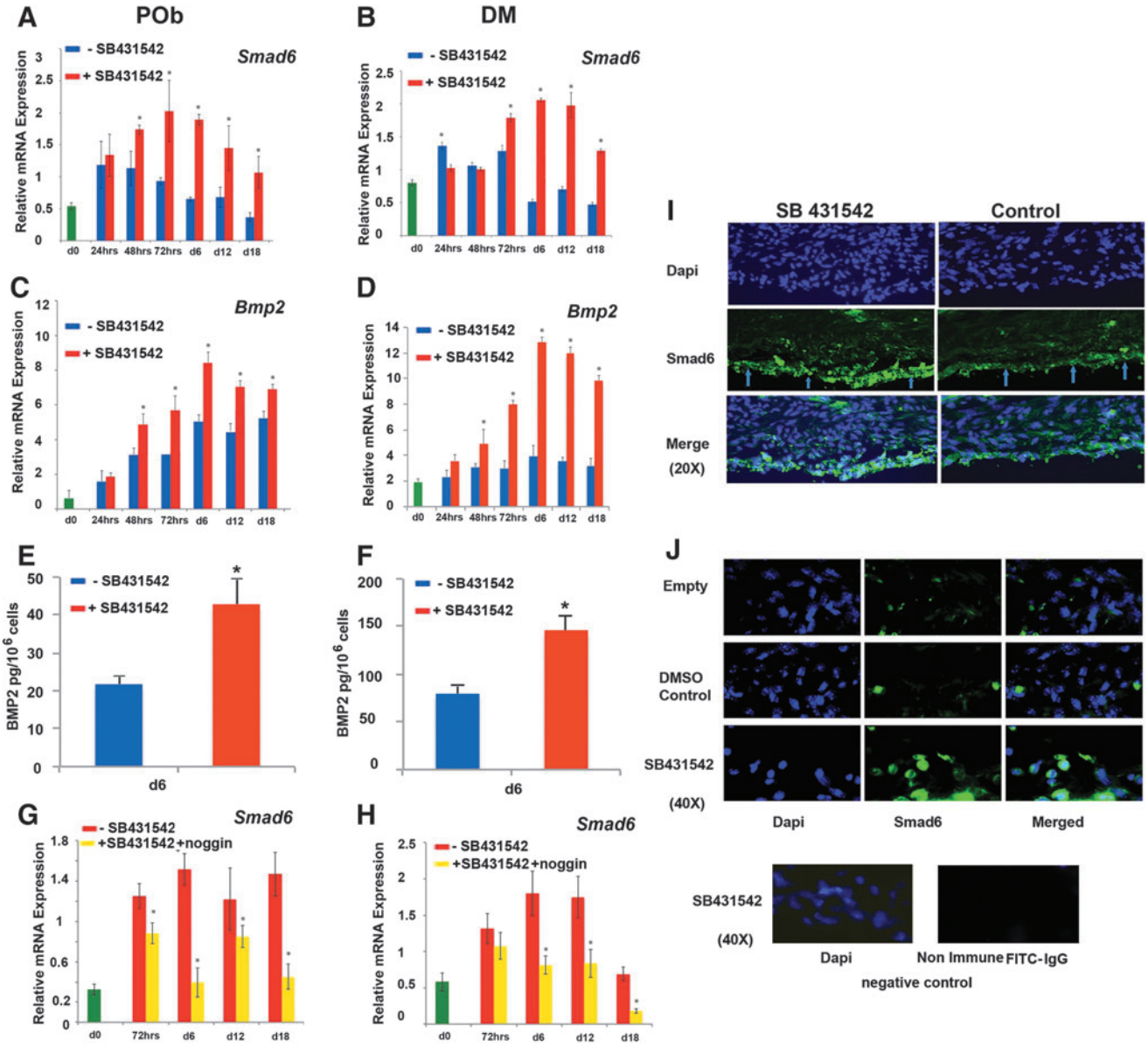

FIG. 5. Small molecule inhibition of TGFβ signaling using SB431542 upregulates *Smad6* and *Bmp2*. **(A)** qPCR analysis performed on POb cells undergoing osteogenic differentiation reveals that inhibition of TGFβ by SB431542 treatment significantly upregulates *Smad6* expression. **(B)** qPCR analysis on DM cells showing a similar upregulation of *Smad6* in SB431542-treated cells. **(C)** SB431542 treatment also increases *Bmp2* expression in POb cells, as revealed by qPCR analysis. **(D)** qPCR analysis shows that the *Bmp2* expression profile in SB431542-treated DM cells mirrors that observed in treated POb cells. **(E)** BMP2 immunodetection by ELISA at day 6 of osteogenic differentiation confirms significantly higher levels of BMP2 in SB431542-treated POb cells than in untreated cells. **(F)** ELISA reveals higher levels of BMP2 also in SB431542-treated DM cells. **(G)** qPCR analysis showing that noggin abrogates the upregulation of *Smad6* observed in SB431542-treated POb cells. **(H)** Similarly, noggin suppresses *Smad6* upregulation in SB431542-treated DM cells. **(I)** Immunofluorescence staining for Smad6 performed on coronal sections through DM spanning the calvarial defect (day 6 postsurgery) shows larger number of DM cells (*arrows*) with strong nuclear staining in SB431542-treated calvarial defects than control (DMSO). Empty is untreated defect without sponge. Magnification at 20×. **(J)** Images taken at 40× magnification. As negative control, a primary (irrelevant) rabbit IgG antibody was used followed by incubation with Alexa Fluor 488 goat antirabbit IgG secondary antibody. Specimen used as negative control was a coronal section of SB431542-treated calvarial defects. $*p \leq 0.05$. Color images available online at www.liebertpub.com/tea

Previously, Schindeler *et al.* showed increased expression of osteogenic markers in SB431542-treated MC3t3-E1 murine preosteoblast cell line, whereas systemic administration did not lead to increased intramedullary bone formation in a model after marrow ablation and intramedullary reaming.[56] The choice of a long bone model in this previous study, rather than a calvarial model, may account for differences in local availability of osteoprogenitors, and, therefore, may be a possible explanation for the disparity with our findings.

Several reports indicated that DM cells play a key role in calvarial skeletal repair. These cells are highly proliferative after the creation of calvarial defects and migrating into the

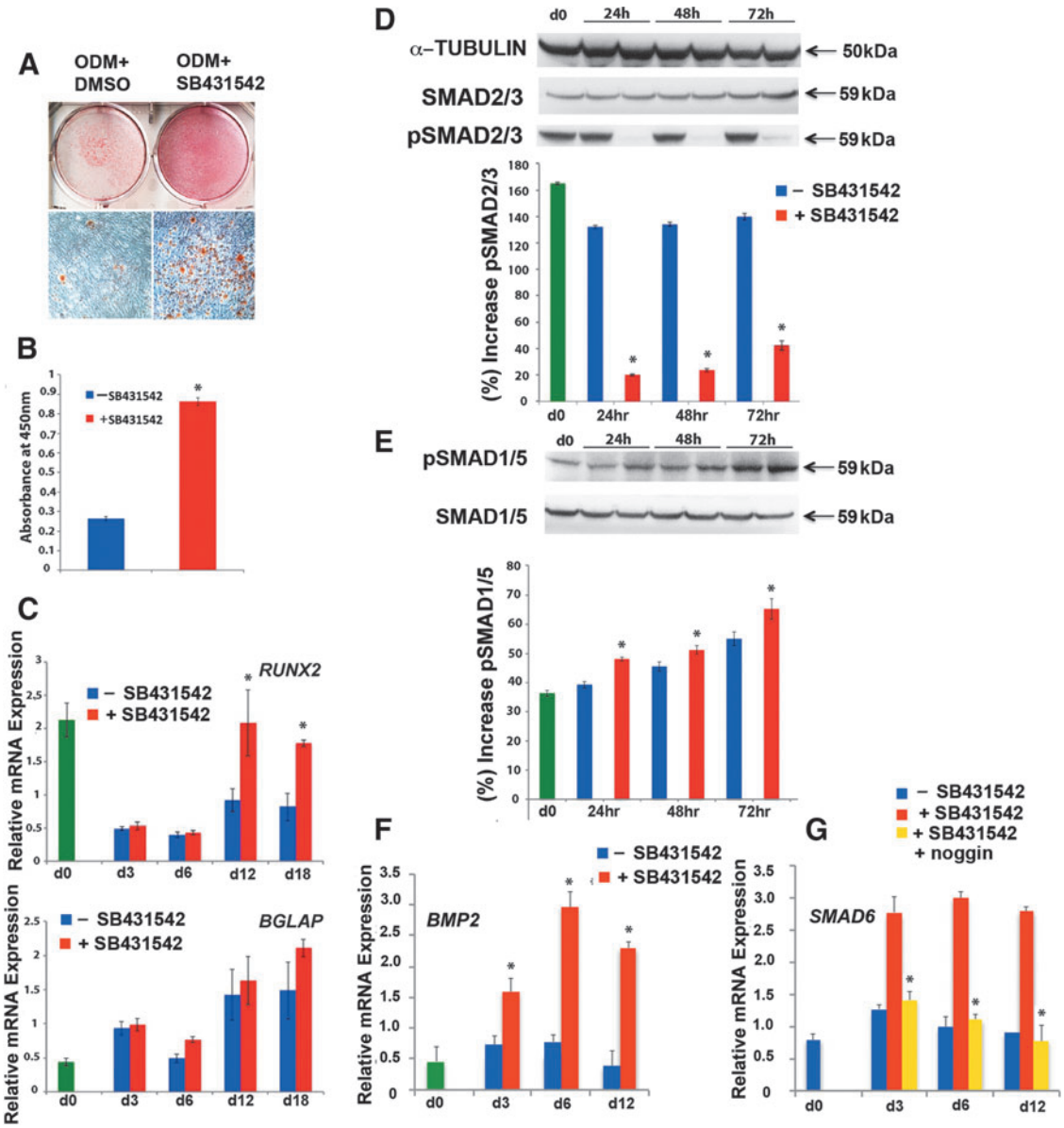

FIG. 6. Small molecule inhibition of TGFβ signaling using SB431542 on primary human POb cells enhances osteogenic capacity and leads to increased BMP signaling through cross-talk. **(A)** Mineralization of the extracellular matrix detected by alizarin red staining demonstrates a significant increase in osteogenesis in primary hPOb cells treated with SB431542 as compared with controls. **(B)** Histogram represents alizarin red staining quantification. **(C)** PCR analysis indicates that treatment with SB431542 upregulates *RUNX2* and *BGLAP* expression. The relative mRNA level in each sample is normalized to *GAPDH* and values are given relative to *GAPDH* expression. $*p \leq 0.05$. **(D)** and **(E)** Immunoblotting analysis of pSMAD2/3 and pSMAD1/5 performed on cells during osteogenic differentiation demonstrates that SB431542 treatment effectively inhibits TGFβ signaling while increasing BMP signaling in hPOb cells at the 24, 48, and 72 h time points. Histograms represent quantification of pSMAD2/3 and pSMAD1/5 electrophoretic bands using densitometry analysis by ImageJ software. Membranes were stripped and reprobed with α–tubulin antibody to control for equal loading. Total SMAD2 and SMAD5 proteins were detected by specific pan SMAD2/3 and SMAD1/5 antibodies. **(F)** PCR analysis reveals that SB431542-treated cells express significantly more *BMP2*. **(G)** PCR showing that increased expression of *BMP2* is paralleled by upregulation of *SMAD6* in SB431542-treated cells with noggin treatment abrogating this upregulation. $*p \leq 0.05$. hPOb, human parietal osteoblasts. Color images available online at www.liebertpub.com/tea

site of the healing defect to contribute to skeletal repair.[14] Gosain *et al.* using a polytetrafluoroethylene barrier to shield either the DM or the pericranium from the site of a calvarial defect created in rabbit, demonstrated that DM was the main source of cells contributing to repairing the defect.[50]

In our calvarial defect model, where great care is taken to preserve the underlying DM, the need for local recruitment of osteoprogenitors for which TGFβ signaling is required may be less pressing because of abundant local availability of osteoprogenitors in the DM. In this context, the effect of SB431542 on promoting terminal differentiation and matrix mineralization phases of differentiation might play the dominant role over osteoprogenitor recruitment, unlike in long bone injury models. Furthermore, given that the

DM cells express high levels of TGFβ (Supplementary Fig. S1D), inhibition of this pathway will have a heightened pro-osteogenic effect by promoting osteoblastic differentiation of osteoprogenitors within this layer.

Using DM cells, we also established that SB431542 treatment enhanced osteogenesis relative to controls. Although there was no significant difference in *Runx2* expression, there was significantly increased *Bglap* expression in the maturation phase, supporting previous findings on the role of SB431542 in the late phases of differentiation.[52] Apoptotic activity of DM cells undergoing osteogenic differentiation was also significantly reduced, mirroring the earlier finding in parietal osteoblasts.[16]

We investigated next whether a cross-talk between TGFβ and BMP signaling would be the mechanism for the observed increase in osteogenic capacity. Analysis for endogenous pSmad2 performed on both DM cells and POb cells during osteogenic differentiation indicated that suppression of pSmad2/3 levels by SB431542 at 24 and 48 h was paralleled by increase in endogenous pSmad1/5, signifying activation of BMP signaling, and, therefore, the presence of a cross-talk more prominent at early time points. The effects at 72 h and day 6 were not significant and appeared to follow a waning BMP response after the 48-h time point. Cross-talk between the TGFβ and BMP pathways was also confirmed *in vivo* by immunofluoresence performed on calvarial defects, showing that a rapid effective supression of TGFβ signaling in the SB431542-treated group was paralleled by a prolonged activation of BMP signaling. Thus, upon TGFβ inhibition with SB431542, there is a release from this natural rheostat on BMP signaling, leading to a prolonged response and, therefore, faster and more robust *in vivo* calvarial regeneration.

To investigate the potential translational benefit of SB431542 treatment in human bone repair, we tested the effect of SB431542 on primary human parietal osteoblasts. The results indicated that SB431542 enhances osteogenesis in a molecular manner similar to that observed in mouse.

Our investigation into the potential molecular mechanism(s) for cross-talk began with analysis for *Smad6* expression to test whether a downregulation of this inhibitory Smad would be responsible for mediating cross-talk between the TGFβ and BMP pathways as previously reported.[52] The initial hypothesis was that a reduction in *Smad6* expression, as a result of TGFβ inhibition with SB431542, might be responsible for activation of BMP signaling. Administration of SB431542, however, led to an unexpected rise in *Smad6* in both DM cells and osteoblasts, thereby ruling it out as a possible mechanism for cross-talk in our study. The disparity between ours and previous findings,[52] however, may well reflect differences between the immortilized C2C12 cells used in the previous study and our cells that are primary cells. Interestingly, we found that increased levels of BMP2 in cells treated with SB431542 to be responsible for *Smad6* upregulation as indicated by suppression of this response with noggin treatment. Taken together, these data suggest that *Smad6* is not responsible for the cross-talk between the TGFβ and BMP pathways, but rather is upregulated in response to enhanced BMP activity in SB431542-treated cells. Smad6, therefore, fine-tunes BMP signaling activity through a negative feedback loop to contain excessive BMP signaling (Fig. 7). The mechanism(s) highlighted in this study represent an opportunity to optimize and/or potentiate the osteogenic fate of other cells, likely adipose-derived stem cells, for their use in bone-regenerative medicine.

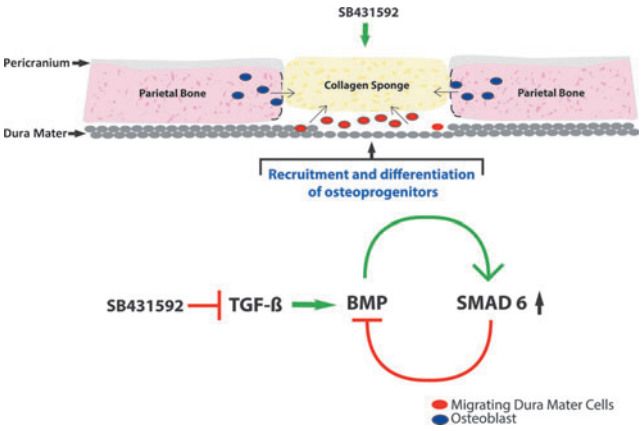

FIG. 7. Cartoon depicting schematically the proposed underlying molecular mechanism(s) governing the healing of calvarial defects treated with SB431542. Inhibition of TGFβ signaling by SB431542 treatment leads to activation of BMP signaling through stimulation of the pro-osteogenic BMP2 ligand production in DM cells migrating into the area of defect. These cells from an immature status promptly differentiate along the osteogenic lineage, thus participating in the healing of bone. Furthermore, SB431542 upregulates inhibitory Smad6 in response to elevated BMP2, thus providing a negative feedback loop to contain excessive BMP signaling. Color images available online at www.liebertpub.com/tea

In conclusion, our study demonstrates that SB431542-induced TGFβ inhibition promotes calvarial regeneration by potentiation and prolongation of the BMP signaling response to injury and possibly by reducing apoptotic activity. Furthermore, the conservation of these mechanism(s) in human calvarial osteoblasts points to the possibility that small molecule modulation of TGFβ signaling may be a viable therapeutic approach either in isolation or as adjunct to conventional therapies for large calvarial defects. This approach could also conceivably be used as an adjunct to novel cellular therapeutic approaches. Collectively, these data set the stage for potential translational applications of small molecules for skeletal repair.

Acknowledgments

This work was supported by the Oak Foundation, the Gunn/Olivier fund, the Hagey Laboratory for Pediatric Regenerative Medicine, and the National Institutes of Health NIH grants R01 DE021683-01, R01 DE19434, U01HL099776 to M.T.L.; ''Transplant and Tissue Engineering Program Endowment Awards'' Lucille Packard Children Hospital Translational Medicine/Transplant'' Stanford University, Child Health Research Institute Fellowship, Stanford University to K.S.-Y.; Medical Research Council Grant MR/L017237/1 to K.S.-Y. and K.J.L.

Author Contributions

K.S.-Y.: collection and assembly of data, data analysis, article writing, final approval of article; S.L.: data analysis, final approval of article; E.Z.:assembly of data, final approval of article; G.W. & K.P.: collection and assembly of

data; J.B. & A.G.: final approval of article; D.C.W.: collection of data, final approval of article; K.J.L.: financial support, final approval of article; M.T.L.: financial support, final approval of article; N.Q.: conception and design, collection and assembly of data, data analysis, writing/editing of article, final approval of article.

Disclosure Statement

No competing financial interests exist.

References

1. Amini, A.R., Laurencin, C.T., and Nukavarapu, S.P. Bone tissue engineering: recent advances and challenges. Crit Rev Biomed Eng **40,** 363, 2012.
2. Baroli, B. From natural bone grafts to tissue engineering therapeutics: brainstorming on pharmaceutical formulative requirements and challenges. J Pharm Sci **98,** 1317, 2009.
3. Steiner, C., Elixhauser, A., and Schnaier, J. The healthcare cost and utilization project: an overview. Eff Clin Pract **5,** 143, 2002.
4. Shenaq, S.M. Reconstruction of complex cranial and craniofacial defects utilizing iliac crest-internal oblique microsurgical free flap. Microsurgery **9,** 154, 1988.
5. Rah, D.K. Art of replacing craniofacial bone defects. Yonsei Med J **41,** 756, 2000.
6. Bruens, M.L., Pieterman, H., de Wijn, J.R., and Vaandrager, J.M. Porous polymethylmethacrylate as bone substitute in the craniofacial area. J Craniofac Surg **14,** 63, 2003.
7. St John, T.A., Vaccaro, A.R., Sah, A.P., Schaefer, M., Berta, S.C., Albert, T., and Hilibrand, A. Physical and monetary costs associated with autogenous bone graft harvesting. Am J Orthop (Belle Mead NJ) **32,** 18, 2003.
8. Karsenty, G. Minireview: transcriptional control of osteoblast differentiation. Endocrinology **142,** 2731, 2001.
9. Karsenty, G. Transcriptional control of skeletogenesis. Annu Rev Genomics Hum Genet **9,** 183, 2008.
10. Jiang, X., Iseki, S., Maxson, R.E., Sucov, H.M., and Morriss-Kay, G.M. Tissue origins and interactions in the mammalian skull vault. Dev Biol **241,** 106, 2002.
11. Quarto, N., Wan, D.C., Kwan, M.D., Panetta, N.J., Li, S., and Longaker, M.T. Origin matters: differences in embryonic tissue origin and Wnt signaling determine the osteogenic potential and healing capacity of frontal and parietal calvarial bones. J Bone Miner Res **25,** 1680, 2010.
12. Li, S., Quarto, N., and Longaker, M.T. Activation of FGF signaling mediates proliferative and osteogenic differences between neural crest derived frontal and mesoderm parietal derived bone. PLoS One **5,** e14033, 2010.
13. Quarto, N., Behr, B., Li, S., and Longaker, M.T. Differential FGF ligands and FGF receptors expression pattern in frontal and parietal calvarial bones. Cells Tissues Organs **190,** 158, 2009.
14. Behr, B., Panetta, N.J., Longaker, M.T., and Quarto, N. Different endogenous threshold levels of Fibroblast Growth Factor-ligands determine the healing potential of frontal and parietal bones. Bone **47,** 281, 2010.
15. Senarath-Yapa, K., Li, S., Meyer, N.P., Longaker, M.T., and Quarto, N. Integration of multiple signaling pathways determines differences in the osteogenic potential and tissue regeneration of neural crest-derived and mesoderm-derived calvarial bones. Int J Mol Sci **14,** 5978, 2013.
16. Li, S., Meyer, N.P., Quarto, N., and Longaker, M.T. Integration of multiple signaling regulates through apoptosis the differential osteogenic potential of neural crest-derived and mesoderm-derived Osteoblasts. PLoS One **8,** e58610, 2013.
17. Inman, G.J., Nicolas, F.J., Callahan, J.F., Harling, J.D., Gaster, L.M., Reith, A.D., Laping, N.J., and Hill, C.S. SB-431542 is a potent and specific inhibitor of transforming growth factor-beta superfamily type I activin receptor-like kinase (ALK) receptors ALK4, ALK5, and ALK7. Mol Pharmacol **62,** 65, 2002.
18. Bonewald, L.F., and Dallas, S.L. Role of active and latent transforming growth factor beta in bone formation. J Cell Biochem **55,** 350, 1994.
19. Robey, P.G., Young, M.F., Flanders, K.C., Roche, N.S., Kondaiah, P., Reddi, A.H., Termine, J.D., Sporn, M.B., and Roberts, A.B. Osteoblasts synthesize and respond to transforming growth factor-type beta (TGF-beta) in vitro. J Cell Biol **105,** 457, 1987.
20. Dallas, S.L., Sivakumar, P., Jones, C.J., Chen, Q., Peters, D.M., Mosher, D.F., Humphries, M.J., and Kielty, C.M. Fibronectin regulates latent transforming growth factor-beta (TGF beta) by controlling matrix assembly of latent TGF beta-binding protein-1. J Biol Chem **280,** 18871, 2005.
21. Ignotz, R.A., and Massague, J. Cell adhesion protein receptors as targets for transforming growth factor-beta action. Cell **51,** 189, 1987.
22. Noda, M., and Camilliere, J.J. In vivo stimulation of bone formation by transforming growth factor-beta. Endocrinology **124,** 2991, 1989.
23. Zhang, H., Ahmad, M., and Gronowicz, G. Effects of transforming growth factor-beta 1 (TGF-beta1) on in vitro mineralization of human osteoblasts on implant materials. Biomaterials **24,** 2013, 2003.
24. Srouji, S., Blumenfeld, I., Rachmiel, A., and Livne, E. Bone defect repair in rat tibia by TGF-beta1 and IGF-1 released from hydrogel scaffold. Cell Tissue Bank **5,** 223, 2004.
25. Ripamonti, U., Ferretti, C., Teare, J., and Blann, L. Transforming growth factor-beta isoforms and the induction of bone formation: implications for reconstructive craniofacial surgery. J Craniofac Surg **20,** 1544, 2009.
26. Tachi, K., Takami, M., Sato, H., Mochizuki, A., Zhao, B., Miyamoto, Y., Tsukasaki, H., Inoue, T., Shintani, S., Koike, T., Honda, Y., Suzuki, O., Baba, K., and Kamijo, R. Enhancement of bone morphogenetic protein-2-induced ectopic bone formation by transforming growth factor-beta1. Tissue Eng Part A **17,** 597, 2011.
27. Lind, M. Growth factor stimulation of bone healing. Effects on osteoblasts, osteomies, and implants fixation. Acta Orthop Scand Suppl **283,** 2, 1998.
28. Alliston, T., Choy, L., Ducy, P., Karsenty, G., and Derynck, R. TGF-beta-induced repression of CBFA1 by Smad3 decreases cbfa1 and osteocalcin expression and inhibits osteoblast differentiation. EMBO J **20,** 2254, 2001.
29. Erlebacher, A., and Derynck, R. Increased expression of TGF-beta 2 in osteoblasts results in an osteoporosis-like phenotype. J Cell Biol **132,** 195, 1996.
30. Heldin, C.H., Miyazono, K., and ten Dijke, P. TGF-beta signalling from cell membrane to nucleus through SMAD proteins. Nature **390,** 465, 1997.
31. Derynck, R., and Zhang, Y.E. Smad-dependent and Smad-independent pathways in TGF-beta family signalling. Nature **425,** 577, 2003.
32. Shi, Y., and Massague, J. Mechanisms of TGF-beta signaling from cell membrane to the nucleus. Cell **113,** 685, 2003.

33. Piek, E., Heldin, C.H., and Ten Dijke, P. Specificity, diversity, and regulation in TGF-beta superfamily signaling. FASEB J **13,** 2105, 1999.
34. Wallace, E.M., Lyssikatos, J.P., Yeh, T., Winkler, J.D., and Koch, K. Progress towards therapeutic small molecule MEK inhibitors for use in cancer therapy. Curr Top Med Chem **5,** 215, 2005.
35. Blake, R.A., Broome, M.A., Liu, X., Wu, J., Gishizky, M., Sun, L., and Courtneidge, S.A. SU6656, a selective src family kinase inhibitor, used to probe growth factor signaling. Mol Cell Biol **20,** 9018, 2000.
36. Hong, C.C., and Yu, P.B. Applications of small molecule BMP inhibitors in physiology and disease. Cytokine Growth Factor Rev **20,** 409, 2009.
37. Tanaka, H., Shinto, O., Yashiro, M., Yamazoe, S., Iwauchi, T., Muguruma, K., Kubo, N., Ohira, M., and Hirakawa, K. Transforming growth factor beta signaling inhibitor, SB-431542, induces maturation of dendritic cells and enhances anti-tumor activity. Oncol Rep **24,** 1637, 2010.
38. Takeuchi, K., Abe, M., Hiasa, M., Oda, A., Amou, H., Kido, S., Harada, T., Tanaka, O., Miki, H., Nakamura, S., Nakano, A., Kagawa, K., Yata, K., Ozaki, S., and Matsumoto, T. Tgf-Beta inhibition restores terminal osteoblast differentiation to suppress myeloma growth. PLoS One **5,** e9870, 2010.
39. Waghabi, M.C., de Souza, E.M., de Oliveira, G.M., Keramidas, M., Feige, J.J., Araujo-Jorge, T.C., and Bailly, S. Pharmacological inhibition of transforming growth factor beta signaling decreases infection and prevents heart damage in acute Chagas' disease. Antimicrob Agents Chemother **53,** 4694, 2009.
40. Cabello-Verrugio, C., Cordova, G., Vial, C., Zuniga, L.M., and Brandan, E. Connective tissue growth factor induction by lysophosphatidic acid requires transactivation of transforming growth factor type beta receptors and the JNK pathway. Cell Signal **23,** 449, 2011.
41. Sugiyama, K., Ishii, G., Ochiai, A., and Esumi, H. Improvement of the breaking strength of wound by combined treatment with recombinant human G-CSF, recombinant human M-CSF, and a TGF-beta1 receptor kinase inhibitor in rat skin. Cancer Sci **99,** 1021, 2008.
42. Nakamura, R., Kayamori, K., Oue, E., Sakamoto, K., Harada, K., and Yamaguchi, A. Transforming growth factor-beta synthesized by stromal cells and cancer cells participates in bone resorption induced by oral squamous cell carcinoma. Biochem Biophys Res Commun **458,** 777, 2015.
43. Cowan, C.M., Shi, Y.Y., Aalami, O.O., Chou, Y.F., Mari, C., Thomas, R., Quarto, N., Contag, C.H., Wu, B., and Longaker, M.T. Adipose-derived adult stromal cells heal critical-size mouse calvarial defects. Nat Biotechnol **22,** 560, 2004.
44. Quarto, N., Wan, D.C., and Longaker, M.T. Molecular mechanisms of FGF-2 inhibitory activity in the osteogenic context of mouse adipose-derived stem cells (mASCs). Bone **42,** 1040, 2008.
45. Levi, B., Hyun, J.S., Nelson, E.R., Li, S., Montoro, D.T., Wan, D.C., Jia, F.J., Glotzbach, J.C., James, A.W., Lee, M., Huang, M., Quarto, N., Gurtner, G.C., Wu, J.C., and Longaker, M.T. Nonintegrating knockdown and customized scaffold design enhances human adipose-derived stem cells in skeletal repair. Stem Cells **29,** 2018, 2011.
46. Quarto, N., Senarath-Yapa, K., Renda, A., and Longaker, M.T. TWIST1 silencing enhances in vitro and in vivo osteogenic differentiation of human adipose-derived stem cells by triggering activation of BMP-ERK/FGF signaling and TAZ upregulation. Stem Cells **33,** 833, 2015.
47. Quarto, N., Li, S., Renda, A., and Longaker, M.T. Exogenous activation of BMP-2 signaling overcomes TGFbeta-mediated inhibition of osteogenesis in Marfan embryonic stem cells and Marfan patient-specific induced pluripotent stem cells. Stem Cells **30,** 2709, 2012.
48. Russell, H.K., Jr. A modification of Movat's pentachrome stain. Arch Pathol **94,** 187, 1972.
49. Behr, B., Sorkin, M., Lehnhardt, M., Renda, A., Longaker, M.T., and Quarto, N. A comparative analysis of the osteogenic effects of BMP-2, FGF-2, and VEGFA in a calvarial defect model. Tissue Eng Part A **18,** 1079, 2012.
50. Gosain, A.K., Santoro, T.D., Song, L.S., Capel, C.C., Sudhakar, P.V., and Matloub, H.S. Osteogenesis in calvarial defects: contribution of the dura, the pericranium, and the surrounding bone in adult versus infant animals. Plast Reconstr Surg **112,** 515, 2003.
51. Wang, J., and Glimcher, M.J. Characterization of matrix-induced osteogenesis in rat calvarial bone defects: II. Origins of bone-forming cells. Calcif Tissue Int **65,** 486, 1999.
52. Maeda, S., Hayashi, M., Komiya, S., Imamura, T., and Miyazono, K. Endogenous TGF-beta signaling suppresses maturation of osteoblastic mesenchymal cells. EMBO J **23,** 552, 2004.
53. Miyazono, K., and Miyazawa, K. Id: a target of BMP signaling. Sci STKE **2002,** pe40, 2002.
54. Ishida, W., Hamamoto, T., Kusanagi, K., Yagi, K., Kawabata, M., Takehara, K., Sampath, T.K., Kato, M., and Miyazono, K. Smad6 is a Smad1/5-induced smad inhibitor. Characterization of bone morphogenetic protein-responsive element in the mouse Smad6 promoter. J Biol Chem **275,** 6075, 2000.
55. Wang, Q., Wei, X., Zhu, T., Zhang, M., Shen, R., Xing, L., O'Keefe, R.J., and Chen, D. Bone morphogenetic protein 2 activates Smad6 gene transcription through bone-specific transcription factor Runx2. J Biol Chem **282,** 10742, 2007.
56. Schindeler, A., Morse, A., Peacock, L., Mikulec, K., Yu, N.Y., Liu, R., Kijumnuayporn, S., McDonald, M.M., Baldock, P.A., Ruys, A.J., and Little, D.G. Rapid cell culture and pre-clinical screening of a transforming growth factor-beta (TGF-beta) inhibitor for orthopaedics. BMC Musculoskelet Disord **11,** 105, 2010.

Address correspondence to:
Natalina Quarto, PhD
Hagey Laboratory for Pediatric Regenerative Medicine
Department of Surgery
Stanford University School of Medicine
257 Campus Drive
Stanford, CA 94305-2200

E-mail: quarto@unina.it

or

Michael T. Longaker, MD
Hagey Laboratory for Pediatric Regenerative Medicine
Department of Surgery
Stanford University School of Medicine
257 Campus Drive, MC 5148
Stanford, CA 94305-5148

E-mail: longaker@stanford.edu

Received: November 24, 2015
Accepted: March 31, 2016
Online Publication Date: April 27, 2016